AIAA JOURNAL
Vol. 39, No. 7, July 2001

Experimental Study of Sound Generated by Backward-Facing Steps Under Wall Jet

Marc C. Jacob,* Alain Louisot,† and Daniel Juvé‡
Centre National de la Recherche Scientifique, 69131 Ecully Cedex, France
and
Sylvie Guerrand§
Société Nationale des Chemins de Fers Français, 75379 Paris Cedex 08, France

Sound radiation by a backward facing step under a plane wall jet is examined. The investigation is based on an experiment where the mean velocity, the step heights, and the cross-stream extent of the jet are varied. The comparison between the backward-facing-step flow and the corresponding wall jet shows an acoustic source near the step. Both near- and far-field measurements indicate how the step changes the radiation pattern of this source. The sound level is significantly increased into the upstream directions and accompanied by strong low-frequency peaks in the spectra. Aerodynamic results show that the reattachment length is much shorter for a step placed under a wall jet than for a step placed in a channel and that the most turbulent flow regions, namely, the jet mixing layer and the step reattachment region, coincide with the acoustic source locations.

Nomenclature

C	=	far-field array center
c_0	=	speed of sound
e	=	nozzle cross-stream width
h	=	step height
k	=	acoustic wave number
l	=	jet half-width
O	=	coordinate origin
R	=	observation distance from O
R'	=	observation distance from far field array center C
Re_h	=	Reynolds number based step height h and maximal streamwise velocity at $x = 0$, U_{ref}; $U_{\text{ref}}h/\nu$
Re_j	=	Reynolds number based on nozzle cross-stream width e and jet exhaust velocity U_j; $U_j e/\nu$
U, V	=	mean velocity in the x and y directions, respectively
U_j	=	jet outlet velocity
U_m	=	maximal streamwise velocity at a fixed streamwise location
U_{ref}	=	maximal streamwise velocity at $x = 0$; $U_m(x = 0)$
u, v	=	streamwise and cross-stream turbulent velocity fluctuations
u', v'	=	rms values of u and v
X	=	streamwise distance from nozzle
x	=	streamwise coordinate
x_r	=	x coordinate of the reattachment point
y	=	crossflow coordinate
y_m	=	y location where U_m is reached
z	=	spanwise coordinate
θ	=	observation angle with respect to (O, x)
θ'	=	observation angle with respect to (C, x)
ν_0	=	kinematic viscosity

Received 6 November 1998; revision received 7 July 2000; accepted for publication 5 January 2001.

*Assistant Professor, Laboratoire de Mécanique des Fluides et d'Acoustique, Unité Mixte de Recherche CNRS 5509, Ecole Centrale de Lyon, B.P. 163; also Assistant Professor, Institut des Sciences et Technologie de l'Ingénieur de Lyon, Université Claude-Bernard Lyon-I, 43 Bd. du 11 Nov. 1918, 69100 Villeurbanne, France. Member AIAA.

†Research Engineer, Laboratoire de Mécanique des Fluides et d'Acoustique, Unité Mixte de Recherche CNRS 5509, Ecole Centrale de Lyon, B.P. 163; also Research Engineer, Centre Acoustique, Metraflu, 64 ch. des Mouilles, 69130 Ecully, France.

‡Professor, Laboratoire de Mécanique des Fluides et d'Acoustique, Unité Mixte de Recherche CNRS 5509, Ecole Centrale de Lyon, B.P. 163. Member AIAA.

§Research Engineer, Direction de la Recherche et de la Technologie, 45 rue de Londres.

I. Introduction

THE acoustic impact of high-speed trains has recently become an important issue because the speeds of these vehicles range up to 300 km/h (187 mph). At such speeds, aeroacoustic sources due to the flow past geometrical singularities on the train body can play a major role in the noise emission. Among these, the flow past a backward facing step is a basic configuration that will be investigated in the present paper.

The backward-facing step under a turbulent boundary layer in a duct flow has been extensively studied in the past because it is a benchmark for the study of turbulent separated flows. A complete review of the experimental work accomplished until the early 1980s has been published by Eaton and Johnston.[1] These authors show the importance of various parameters (incoming turbulence level, boundary-layer thickness, aspect ratio between channel cross stream extent and step height, etc.) in the reattachment process. They also point out that large three-dimensional structures are generated in the recirculation region downstream of the step. Eaton and Johnston[2] also show that the free shear layer downstream of the step undergoes a low-frequency nonperiodic flapping motion that corresponds to Strouhal numbers based on step height and the mean free stream velocity less than 0.02. Its timescale is longer than that of the largest eddies, and no preferred frequency is detected. Careful studies of the low-frequency unsteadiness in other reattaching flow configurations[3] relate this flapping to strength fluctuations and spanwise coherence fluctuations of the large-scale spanwise vortices. However, the origin of these fluctuations is not clearly understood yet. The three-dimensional aspects of the backward-facing-step flows, as well as the related unsteadiness of the separated flow, have been examined in more recent experimental[4] and numerical studies.[5–7] According to these studies, the largest eddies generated in the shear layer are generated at a preferred frequency that corresponds to a Strouhal number between 0.04 and 0.1, which is higher than that of the flapping reported by Eaton and Johnston.[2]

Because they focus on the aerodynamics of separated flows, all of these studies are performed in ducted flows. For acoustic investigations, however, the flow should be surrounded by a medium at rest and an anechoic environment facing the wall containing the step or the far-field measurements. This is probably the reason why so few studies are concerned with the sound generation by a backward-facing step. Classical studies of the sound radiated by a flow past a discontinuous plane concern trailing edges of semi-infinite planes.[8–10] These analytical studies give a good idea how

an eddy interacts with a geometrical singularity to radiate sound, but can not be applied directly to the backward-facing step. Fewer studies relate the sound generated by an eddy in the vicinity of a wedge,[11,12] and to the authors' knowledge there is no literature about sound generation by a backward-facing step, which is expected to behave differently because of its finite height.

Therefore, the sound generation of a turbulent flow past a backward-facing step is investigated in the present paper. To obtain a flow past a step with an acoustic far field in a medium at rest, a turbulent wall jet is chosen instead of a duct flow. In an earlier study,[13] the authors investigated the sound radiated by a turbulent wall jet both experimentally and numerically. The study showed that the major sound sources of such flows are the same as those observed in a freejet (quadrupoles in the mixing region of the jet) but that their propagation is reflected by the wall. Thus, a wall jet can be used for the acoustic characterization of a backward-facing step if the step is not located in the mixing region of the wall jet. In the present paper the sound radiation is related to the separated flow downstream of the step.

II. Experimental Setup

A. Description of the Flow

The experimental setup is shown in Fig. 1, and details are also shown in Fig. 2. Air is supplied at room temperature (15 ± 1°C) in a large anechoic room ($10 \times 8 \times 8$ m^3) by an anechoic wind tunnel. The flow is guided into the room by a 3-m-long square duct (0.5×0.5 m^2 cross section). Then it is accelerated by a convergent nozzle with a rectangular outlet. The spanwise extent is 0.5 m, whereas the nozzle cross-stream width e is either 0.05 m (aspect ratio 10) or 0.025 m (aspect ratio 20). A plane wall jet is then obtained along a plate, which is parallel to the larger side of the nozzle. To avoid spanwise spreading, the wall jet is guided by two lateral walls. The backward-facing step is located 1 m downstream of the nozzle, that is, $20e$ and $40e$ for $e = 0.05$ and 0.025 m, respectively. Downstream of the step, the wall is 2.5 m long for the smaller jet and 3.9 m for the larger one. The objective is to push the end of the plate far enough downstream where the flow is slower and where this spurious noise source does not compete with the investigated sources. In each configuration, the step height h can be varied between 0 and 0.06 m. Thus, the wall jet ($h = 0$) can be taken as a reference for the study of the backward-facing step. The jet exhaust velocity U_j varies between 60 and 140 m/s. The Reynolds number Re_e based on the flow speed, the nozzle cross-stream width e, and the kinematic viscosity $\nu_0 = (1.45 \pm 0.01) \times 10^{-5}$ m^2/s ranges from 1.04×10^5 to 4.83×10^5. The coordinates are x for the streamwise direction, y for the cross-stream direction pointing toward the free boundary, and z for the spanwise direction. The origin is located on the step edge at the half-span. The measurement plane is the $z = 0$ (center) plane. The velocity components corresponding to the x and y directions are, respectively, U and V for the mean flow and u and v for the velocity fluctuations. The spanwise components are not measured in this study.

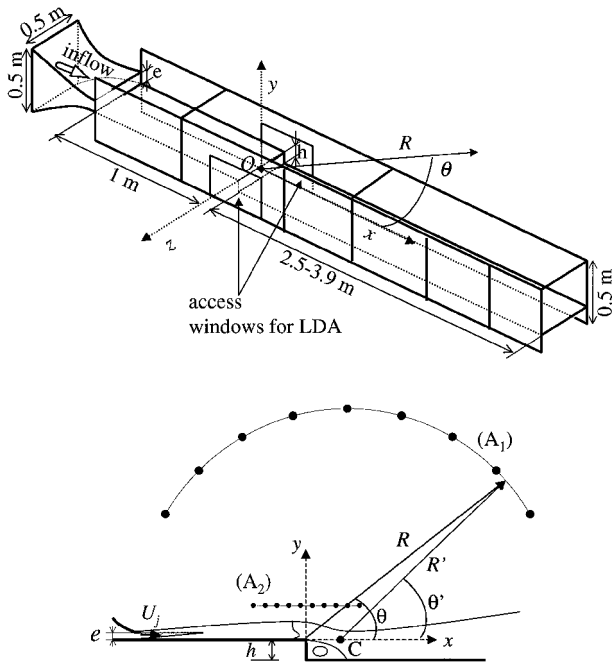

Fig. 1 Experimental setup and coordinate system: A_1 is the far-field array and A_2 the near-field array.

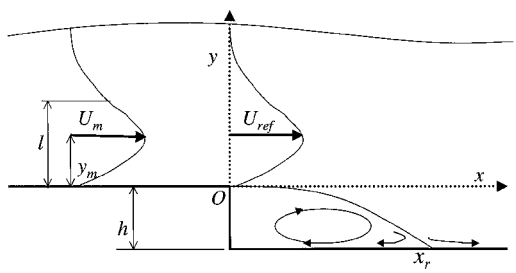

Fig. 2 Schematic view of the step region; $U_{ref} = U_m(x = 0)$.

B. Aerodynamic Measurements

Aerodynamic measurements near the step are carried out with an Aerometrics dual-beam, backward-scatter laser Doppler anemometer (LDA) system. Two pairs of beams are used for two-dimensional velocity measurements. They are supplied by the green line (514.5 nm) and the blue line (488 nm) of a Spectra Physics 4-W argon-ion laser source. The beams of each pair undergo a relative frequency shift of 40 MHz in a Bragg cell. The four beams are guided to the flow with an optical fiber, which is terminated by a focusing lens with a focal length of 500 mm. The beams of each pair have a mutual angle of 7 deg. For the measurement of streamwise and cross-stream velocity components, each laser beam makes a 3.5-deg angle with the z direction in the plane of the corresponding velocity component. The backscattered beams are focused by the same lens and sent through an optical fiber onto photomultipliers. The signals are then treated by two Aerometrics real-time signal analysers and postprocessed on a personal computer. Thus, the lateral walls are locally equipped with 2-cm-thick plexiglass windows. These windows are small (40×30 cm^2) and vertical to avoid their internal stress distribution depolarizing the beams. The seeding material for these high-speed airflows is a mineral oil (paraffin)–trichlorethane mixture. It is injected at 5 hPa through a 50-cm-long tube, which is crossing the centerplane ($z = 0$) 2 m upstream of the nozzle exit. This tube is pierced with 25 equally spaced, 2-mm-wide holes. Thus, particles with a diameter about 1–2 μm are present throughout the flow section in the cross-stream direction y. With this device, no particles are injected into the air entrained by the jet. According to Schneider and Goldstein[14] this results in a slight overestimate of turbulence in the outer part of the flow.

Measurements are carried out for two flow types at 130 m/s with the smaller nozzle ($e = 2.5$ cm): a plane wall jet and a backward facing step ($h = 5$ cm) are examined. The strategy adopted here to verify the LDA and to optimize the acquisition and seeding parameters is the following: The LDA is compared to other LDA measurements and to hot-wire measurements for a flow that is well documented: the plane wall jet.[14] In the present case the flow is studied from the nozzle outlet region to the region where the jet is fully developed (from $x = -20h$ to $-12.5h = -25e$, that is, $15e$ downstream of the nozzle). Then measurements are performed with the step. Measurements are performed from one-step-height usptream to seven-step-heights downstream of the step. Upstream of the step and outside of the recirculating region, it is verified that the LDA data agree with that of a wall jet (obtained both by LDA and hot-wire anemometry). Validation results, which are not reported here, show good agreement with classical hot-wire anemometry.

C. Acoustic Measurements

Acoustic measurements are carried out in the centerplane. The far field is studied with a circular array of nine Bruel and Kjäer $\frac{1}{2}$-in. microphones located $R' = 2.50 \pm 0.01$ m away from a point C located 0.22 m downstream of the step (because the experiment is designed

for a comparison with other flow configurations[15]). Their angle θ' with the downstream x direction varies from 30 to 150 ± 2 deg (every 15 deg). The power spectrum density is computed from 192 Hz to 25.6 kHz every 16 Hz by averaging 100 times series, each being 0.0625 s long and sampled by 4096 points. Lower frequencies (from 0 to 192 Hz) are cut off to meet the far-field requirement, $kR \geq 9$. Thus the directivity is available for various frequency bands, and the overall directivity is computed by integrating the corresponding spectrum. Amplitude corrections are made to center the directivity onto the origin O at a fixed distance $R = 2.5$ m. Corresponding observation angles θ are 28, 42, 56, 70, 85, 100, 115, 131, and 147 deg.

A source localization is performed with a linear near-field array of 10 microphones placed every 7 ± 0.05 cm in parallel to the streamwise direction, 1 m away from the upstream wall ($z = 0$ and $y = 1 \pm 0.002$ m). This array is placed at various streamwise positions, either in the region downstream of the nozzle exit or with its center at the step ($x = 0$), and for each position, a backward-facing-step flow is compared to the corresponding plane wall jet. The localization technique[16] compares the cross-spectrum matrix obtained from the experiment to the matrix constructed from a streamwise distribution of uncorrelated monopoles. An iterative algorithm searches for the best fitting streamwise intensity distribution of monopoles for each frequency from 200 to 5984 Hz. All acoustic signals are treated by a Hewlett–Packard (HP) multichannel data analyzer, which is controlled from a personal computer by HP software. Measurements are carried out at flow speeds ranging from $U_j = 60$ to 140 m/s and for step heights ranging from $h = 0$ to 6 cm.

III. Results

The aerodynamic results are given for a $U_j = 130$ m/s flow over an $h = 5$ cm step and an $e = 2.5$ cm nozzle.

A. Mean Flow

For the backward-facing step, the mean flow can be divided into three regions. Upstream of the step, the flow is that of an unperturbed plane wall jet. Evidence of this is given in Fig. 3, in which velocity profiles upstream of the step are compared to those of a plane wall jet in its self-similar region. At $x = 0$, that is, $40e$ downstream of the nozzle, the maximal streamwise velocity $U_{\max}(x = 0)$ is only 77.4 m/s, less than two-thirds of the outlet velocity U_j: This decrease also compares favorably with the results of Schneider and Goldstein.[14] $U_{\max}(x = 0)$ is taken as reference speed U_{ref} for the step flow, also shown in Fig. 2. The Reynolds number based on h and U_{ref} is $Re_h = 2.58 \times 10^5$. Downstream of the step, the flow is characterized by the typical recirculation bubble (Figs. 4 and 5). Behind the step, negative values of U reach 24% of U_j, that is, 40% of the maximal velocity at the step location U_{ref}. The shear layer reattaches to the wall between $x = 2.75h$ and $3h$, which is a very short distance compared to the reattachment length measured in duct flows. Figure 4

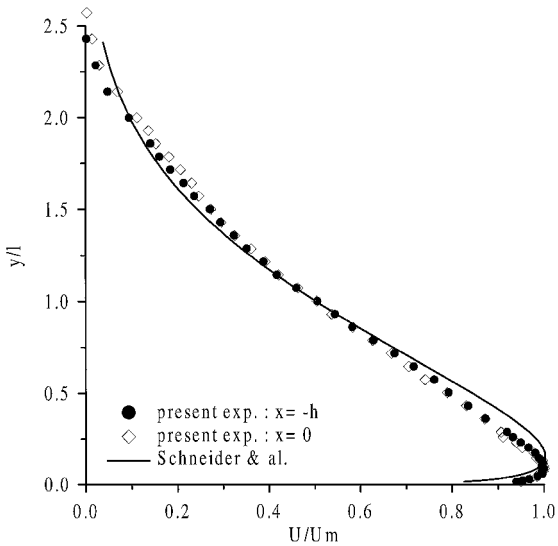

Fig. 3 Incoming wall jet: $U_j = 130$ m/s, $e = 2.5$ cm, $h = 5$ cm, $U_m = 77.4$ m/s, and $l = 1.4h$.

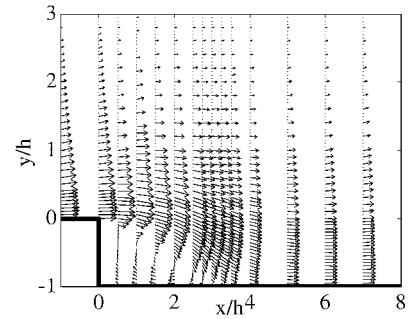

Fig. 4 Mean velocity field near the step: $U_j = 130$ m/s, $e = 2.5$ cm, and $h = 5$ cm.

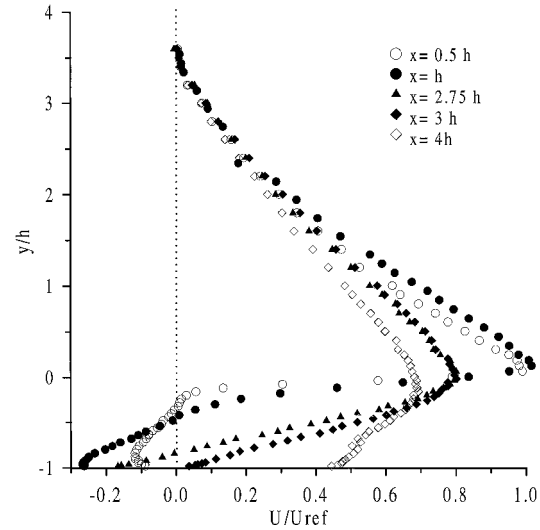

Fig. 5 U profiles downstream of the step: $U_j = 130$ m/s, $U_{\text{ref}} = 77.4$ m/s, $e = 2.5$ cm, and $h = 5$ cm.

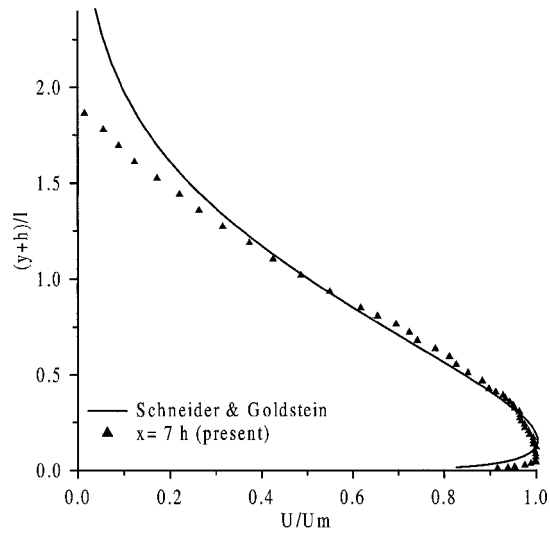

Fig. 6 Wall jet recovery: $U_j = 130$ m/s, $e = 2.5$ cm, $h = 5$ cm, $U_m = 54.3$ m/s, and $l = 2.3h$.

also shows that the jet stops spreading in this region because V becomes negative over almost the whole region (it is only positive in the external part of the flow and near the bottom of the step). Between its reattachment point and $x = 6h$, the flow slowly evolves to a plane wall jet, as shown in Fig. 6, where the profile at $x = 7h$ is compared to the best fit profile of Schneider and Goldstein.[14] There are several reasons for the reattachment length to be so short:

1) The turbulence level of the wall jet (20–30%) is higher than that of a channel flow. Therefore, the cross-stream diffusion of momentum is strongly enhanced.

2) The plane jet over a backward-facing step is governed by three cross-stream scales. The incoming flow has two scales, the

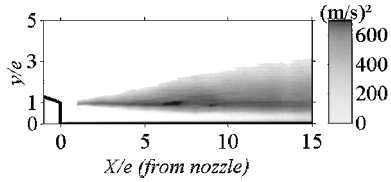

Fig. 7 Distribution of $u'^2 + v'^2$ downstream of the nozzle outlet: U_j = 130 m/s, e = 2.5 cm, and h = 5 cm.

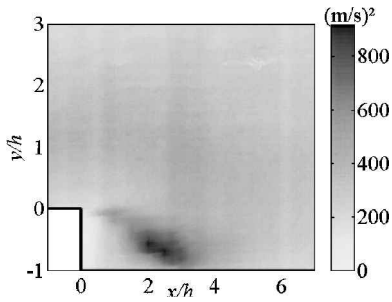

Fig. 8 Distribution of $u'^2 + v'^2$ near the step: U_j = 130 m/s, e = 2.5 cm, and h = 5 cm.

distance from the wall were U_m is reached, y_m, and the jet half-width l (Ref. 17). The step height h is the third essential scale in the reattachment process. When the incoming flow reaches the step, a new shear layer is created, which is governed by the velocity gradient of the upstream flow. The jet half-width l measures the inertia of the incoming flow, whereas y_m measures the wall bounded viscosity against the jet momentum. A small value of l facilitates the bending of this shear layer toward the wall. Therefore, for a given step height h, the reattachment length is shorter in this case than for a backward-facing step in a duct (in means of streamwise momentum, l has to be compared to the duct diameter).

3) The reattachment behind the step is delayed by increasing the expansion ratio in the case of a channel flow. (Because of the resulting adverse pressure gradient, some experiments even show a separation on the opposite wall.[18])

B. Turbulence

Experimental charts of $u'^2 + v'^2$ are plotted on Figs. 7 and 8. Darker areas indicate stronger turbulence levels. There are two regions where the fluctuating velocities are high in this flow. The first is the mixing layer generated at the nozzle outlet, where the maximal turbulence level $\sqrt{(u'^2 + v'^2)}/U_j$ of about 20% is reached about 7e downstream of the nozzle. Furthermore, the level decreases gently and remains fairly high even when the jet reaches the step. (The maximum at $x = 0$ corresponds to a turbulence level of about 15%.) Comparisons with hot-wire anemometry for the wall jet show that the LDA slightly overestimates the turbulence in the outer part of the wall jet shear layer. As mentioned in Sec. II.B and according to Schneider and Goldstein,[14] this can be avoided if the coflow is also seeded, which it is not in the present case. The second highly turbulent region is in the free shear layer generated by the step, with a maximum (the turbulence level is about 39% of U_{ref}, that is, 23% of U_j) just before the reattachment point.

Typical profiles of the streamwise and the cross-stream turbulence downstream of the step are plotted in Figs. 9 and 10; as already mentioned, the velocity scale U_{ref} is the maximal streamwise mean velocity at $x = 0$. Figures 9 and 10 show that u' is about the same order as v' in the outer region but that v' undergoes stronger variations near the wall where it tends to 0. A possible explanation for the small increase of u' in the vicinity of the wall in the recirculation bubble might be due to fluctuations of the reattachment point. This increase is indeed strongest at $x = 3h$ near the mean reattachment point. Turbulence levels u'/U_j in the streamwise direction reach about 17% of U_j just before the reattachment point.

These results show that the two mixing layers are major regions of turbulence. Therefore, strong acoustic sources can be expected in these mixing layers as will be investigated hereafter.

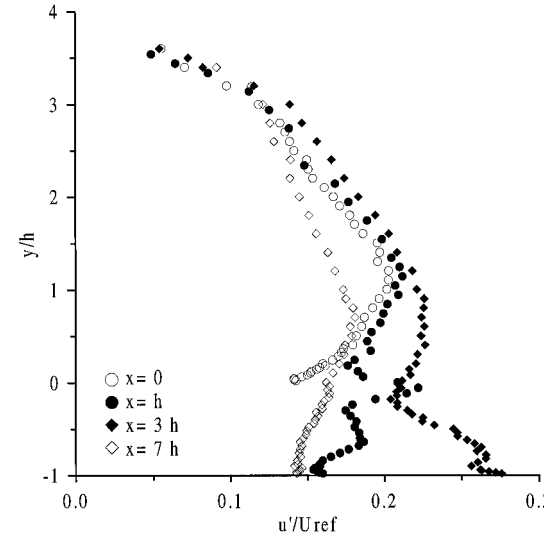

Fig. 9 Streamwise turbulence near the step: U_j = 130 m/s, U_{ref} = 77.4 m/s, e = 2.5 cm, and h = 5 cm.

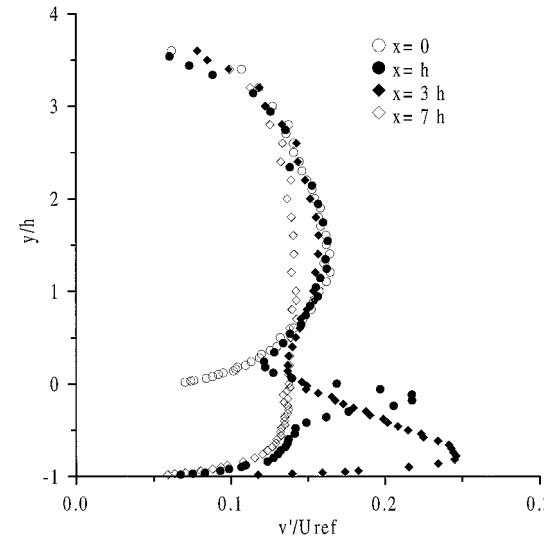

Fig. 10 Cross-stream turbulence near the step: U_j = 130 m/s, U_{ref} = 77.4 m/s, e = 2.5 cm, and h = 5 cm.

C. Source Localizations

The results of the source localizations are shown in the case of a $U_j = 140$ m/s flow over an $h = 4$ cm step, with an $e = 5$ cm nozzle. Figure 11 is obtained with the center of the array facing the step edge. (The center is located at $x = 0$.) Figure 11 represents the streamwise source intensity distribution for frequencies ranging from 200 to 5984 Hz. The decibel scale has an arbitrary reference because the total magnitude of this chart depends on the total acoustic pressure felt by the array but the reference is the same for all charts because the same array is used. The chart gives information of the relative sound power radiated from different source flow cross sections. Figure 11a is obtained without step and Fig. 11b with an $h = 4$ cm step. Because the spatial resolution of the technique is increasing with frequency, the position of the nonnegligible very low-frequency sources ($f < 400$ Hz) cannot be determined precisely. In the present case, the dominant sound source is located slightly downstream of the step, about $2h$–$3h$ downstream and radiates mostly in the lower-frequency range (less than 3–3.5 kHz). The location of the maximal source intensity for each frequency is plotted in Fig. 12 for frequencies ranging from 400 to 5984 Hz. Figure 12 shows that the strongest source is located between $2h$ and $3h$ for frequencies ranging up to 3.5 kHz and $1.5h$ farther downstream at higher frequencies, where the maximal source level is about 20 dB below its highest low-frequency values (according to Fig. 11). Therefore the

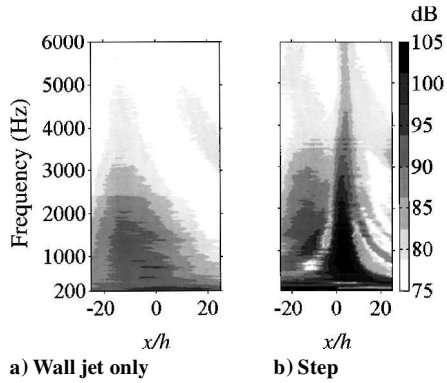

Fig. 11 Source localization (array facing the step): U_j = 140 m/s, e = 5 cm, and h = 4 cm.

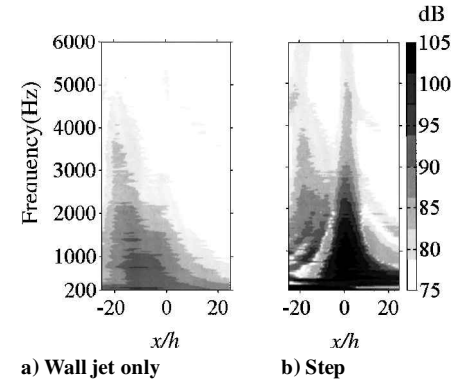

Fig. 13 Source localization (array facing the jet exit zone): U_j = 140 m/s, e = 5 cm, and h = 4 cm.

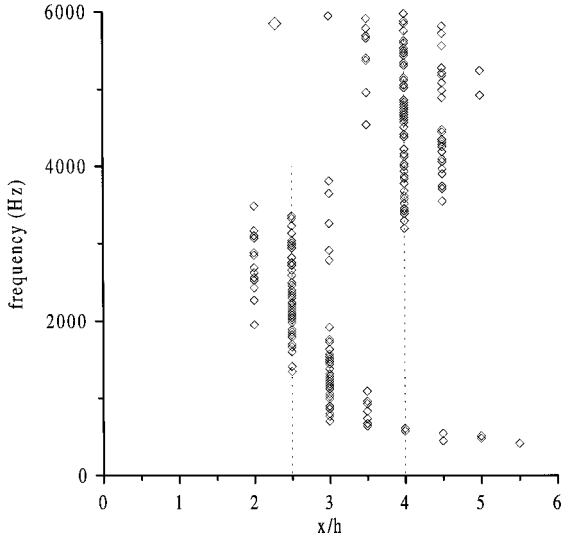

Fig. 12 Location of maximal source vs frequency: U_j = 140 m/s, e = 5 cm, and h = 4 cm; array facing the step.

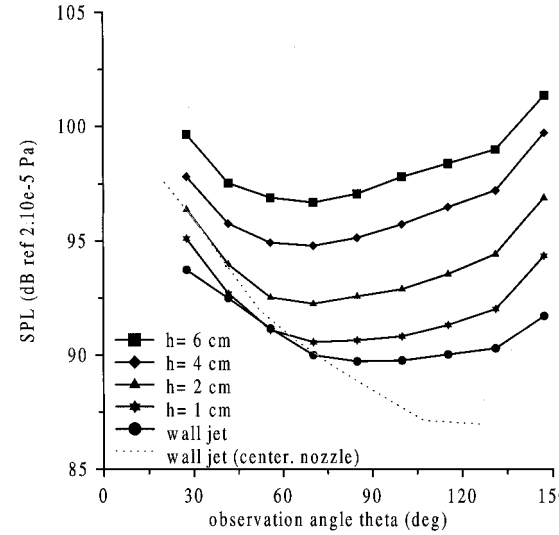

Fig. 14 Far field for various step heights: U_j = 140 m/s and e = 5 cm.

maximal locations at frequencies up to 3.5 kHz, which are about $2.5h$ downstream of the step, indicate the position of the step source. This is where the strongest turbulence levels of the backward-facing-step region are measured.

Another weaker source can be seen upstream of the step in Fig. 11b. A comparison with Fig. 11a shows that this source is due to the wall jet noise. However, because the wall jet sources are concentrated in the jet mixing layer, they are farther from the array than the step source. The microphone that is the most upstream is still about 0.65 m ($13e$) downstream of the nozzle. Thus, the contribution of these sources to the pressure felt by the array is slightly underestimated when compared to the sources that are facing the array, especially the leading step source. To see whether the wall jet source is important compared to the step source, the array is moved upstream so that the upstream microphone is now facing the nozzle outlet. The results of this localization are given in Fig. 13b. Figure 13b clearly shows that the step source is still dominating the wall jet sources, although it is now underestimated. Moreover, the step source location is still correct because of its high intensity. Figure 13a is obtained for the jet alone. It shows that, above very low frequencies, its sources are distributed between the region where the wall jet turbulence level is highest ($x = -18h$, that is, $6e$ downstream of the nozzle) and the step position ($x = 0$). In addition, source levels are decreasing in the downstream direction, as the turbulence level does (Fig. 7). This is in agreement with the fact that the sound production of the wall jet is mostly due to the turbulent eddies produced in its shear layer (see Sec. III.B).

D. Far Field

Figure 14 shows the directivity of the sound pressure level (SPL) for various step heights and for the corresponding wall jet obtained with the large nozzle, all at $U_j = 140$ m/s and $e = 5$ cm. These directivities are centered on the edge of the backward-facing step (see Fig. 1) and are plotted vs θ. Several conclusions can be drawn from Fig. 14: 1) All of the step flows have similar directivities. 2) The radiated sound increases with step height. 3) The sound radiated by the step flow dominates the wall jet radiation and a strong enhancement of both the downstream and upstream directivity appears. 4) The level increase is more pronounced in the upstream directions (70–150 deg). The downstream radiation is found for all jet flows and is not typical of the backward-facing step, but the upstream radiation is. The wall jet also shows a small increase in the upstream directions, but this is just an artifact of the measurements where the dominant jet sources are located closer to the upstream microphones than to the downstream microphones. Evidence of this is shown in the dashed curve of Fig. 14, which is obtained by centering the wall jet directivity on the nozzle outlet (at an 2.5-m distance) with suitable amplitude and angle corrections on the actual measurements. Therefore, it is clear that for a step the level increase in the upstream directions is still stronger than for the wall jet.

The influence of flow speed is shown in Fig. 15, which shows how the flow speed increases the SPL. It appears that the increase is omnidirectional for higher velocities; between 60 and 80 m/s, however, the increase is more pronounced into the directions close to 90 deg. This might be because the wall jet mixing layer noise adds to the step noise and the two sources do not have the same velocity dependence. To find the corresponding power law of this dependence, the directivity of the step source can be isolated from the wall jet noise: In Fig. 16, the equivalent step source contribution is computed for an $h = 4$ cm flow by substracting the mean square pressure of the wall jet from the mean square pressure of the step flow. This is justified by two observations: The step source is apparently not correlated to the wall jet sources, and they both are

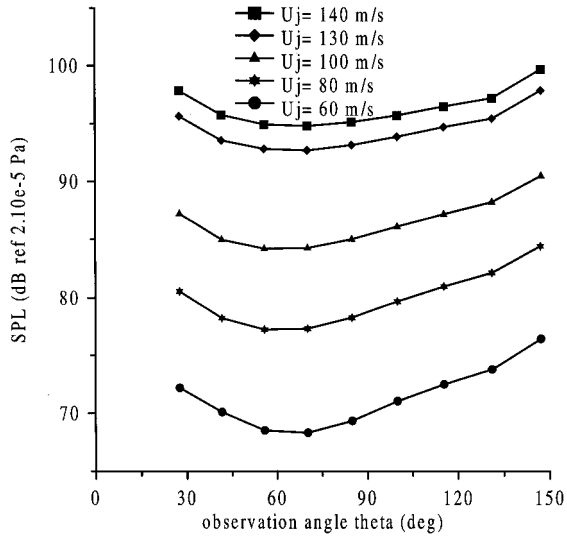

Fig. 15 Influence of U_j onto the total far field: $e = 5$ cm and $h = 4$ cm.

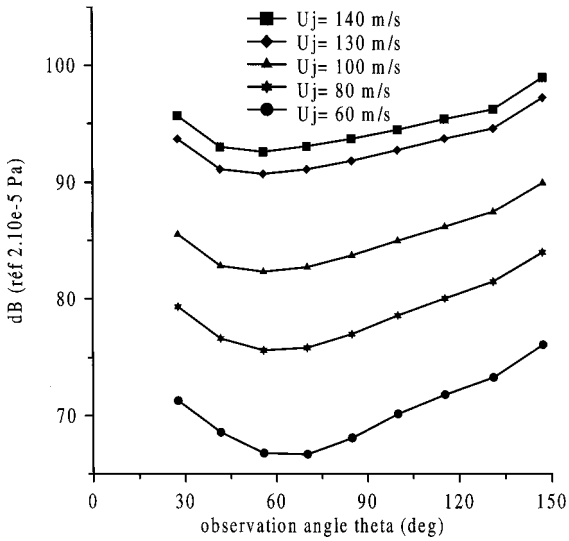

Fig. 16 Influence of U_j onto the step source: $e = 5$ cm and $h = 4$ cm.

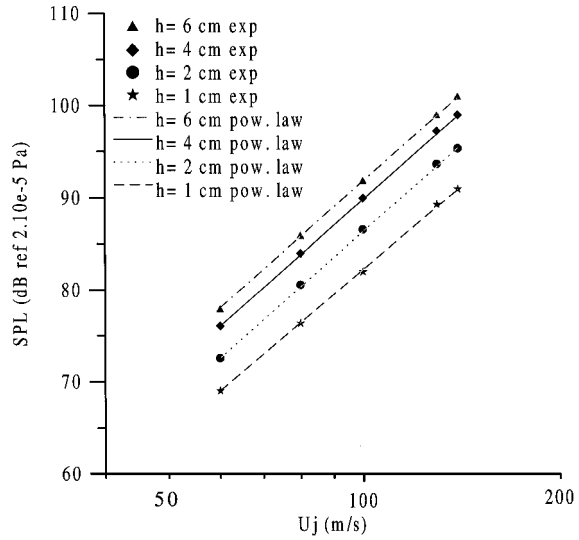

Fig. 17 $U^{6.2}$ power law at $\theta = 147$ deg for various step heights: $e = 5$ cm.

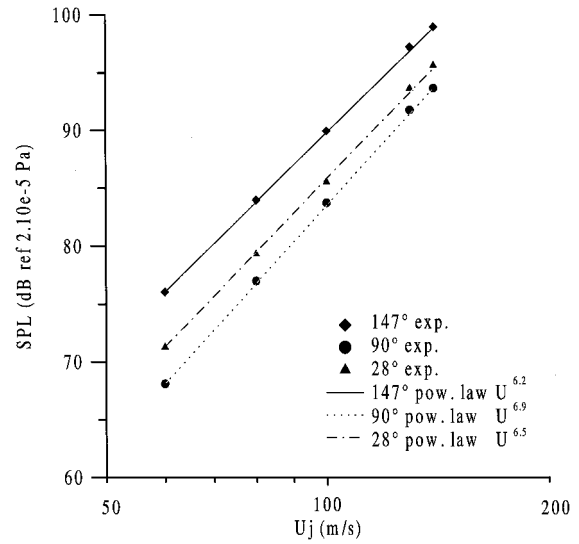

Fig. 18 Power law for an $h = 4$ cm step at various observation angles θ: $e = 5$ cm.

spatially separated. The result confirms the upstream directivity of the step source. In comparison with Fig. 15, the level is decreased by about 2 dB for downstream angles, whereas it remains almost unchanged at high angles. Thus, the radiation at small angles observed in Figs. 14 and 15 is mainly due to the wall jet source. As shown in Fig. 17, the intensity depends on $U_j^{6.1}$ in the direction where the step radiation is the strongest (147 deg), whereas the power increases in other directions as shown in Fig. 18 (it is $U_j^{6.9}$ at 85 deg, where the step source radiation is comparable to the wall jet radiation).

The sound spectra at various observation angles are shown in Fig. 19 for the case where $U_0 = 140$ m/s, $e = 5$ cm, and $h = 4$ cm. All spectra merge for frequencies above 2 kHz. In the low-frequency range, some high level broadband peaks arise for the upstream directions (at 147 deg they are strongest). These peaks have no clear step height dependence and no clear velocity dependence (Figs. 20 and 21). Their characteristic frequencies tend to decrease somewhat with increasing flow speed, but the variations are too small to obtain a constant Strouhal number. The low-frequency peaks are not due to the low-frequency flapping of the separated shear layer because their Strouhal number does not agree with literature (it varies between 0.064 and 0.9 for the 900-Hz peak) and because it is not constant when velocity and step height vary. In the high-frequency range, the spectra have the same shape as the wall jet spectrum, with a higher level (Fig. 20); this overall increase can be explained by the additional eddies generated in the separated flow.

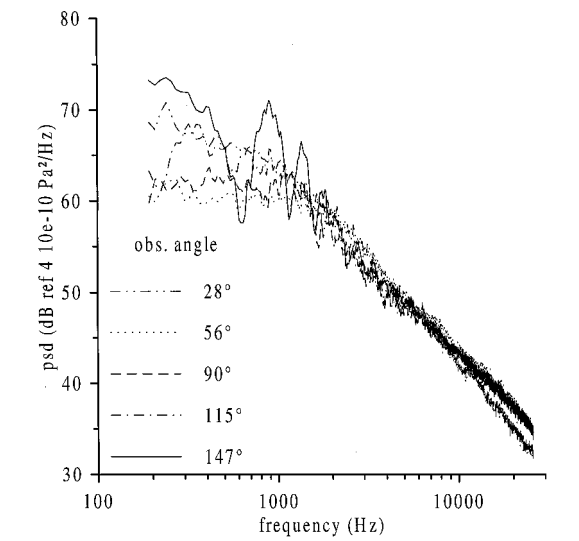

Fig. 19 Power spectrum density at various observation angles θ: $U_j = 140$ m/s, $e = 5$ cm, and $h = 4$ cm.

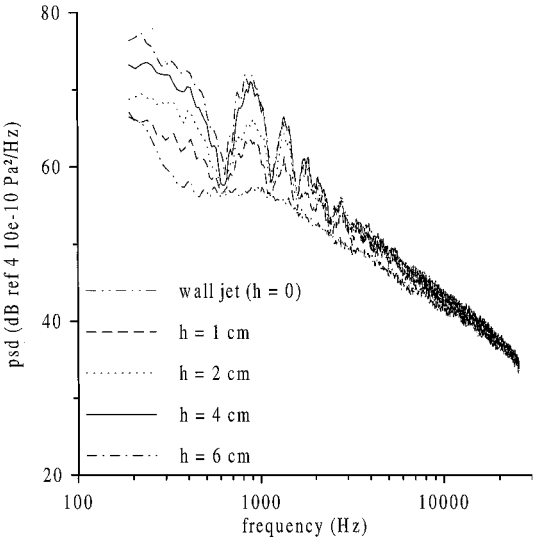

Fig. 20 Power spectrum density at $\theta = 147$ deg for various step heights: $U_j = 140$ m/s and $e = 5$ cm.

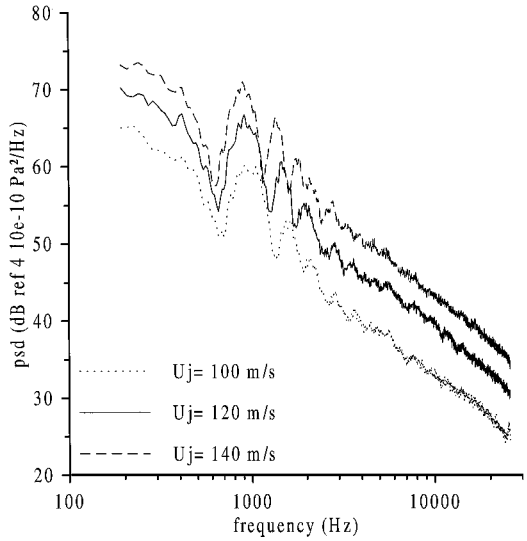

Fig. 21 Power spectrum density at $\theta = 147$ deg for various velocities: $e = 5$ cm and $h = 4$ cm.

IV. Conclusion

An experimental study of the sound generated by a wall jet over a backward-facing step has been carried out and compared to a wall jet. The step has been found to be a major source of noise. It is due to aerodynamic sources generated in the separated flow: The resulting source is located about two step heights downstream of the step in the reattachment region. It has a strong upstream directivity and radiates in the low-frequency range with an intensity that is proportional to $U_j^{6.2}$. The far-field spectrum is characterized by strong peaks in the upstream directions. Their frequencies are almost independent from the step height and the flow velocity, whereas their level increases with these two parameters. The oscillations of the separated shear layer do not seem to contribute significantly to the far field.

Acknowledgments

This work was supported by the French Ministère des Transports. The authors also acknowledge the reviewers for their useful comments.

References

[1]Eaton, J. K., and Johnston, J. P., "A Review on Subsonic Turbulent Flow Reattachment," *AIAA Journal*, Vol. 19, No. 9, 1981, pp. 1093–1099.

[2]Eaton, J. K., and Johnston, J. P., "Low Frequency Unsteadiness of a Reattaching Turbulent Shear Layer," *Proceedings of the Third International Symposium on Turbulent Shear Flows*, 1981, pp. 1617–1622.

[3]Kiya, M., and Sasaki, K., "Structure of Large-Scale Vortices and Unsteady Reverse Flow in the Reattaching Zone of a Turbulent Separation Bubble," *Journal of Fluid Mechanics*, Vol. 154, 1985, pp. 463–491.

[4]Shih, C., and Ho, C. M., "Three-Dimensional Recirculation Flow in a Backward Facing Step," *Journal of Fluids Engineering*, Vol. 116, 1994, pp. 228–232.

[5]Celengil, M. C., and Mellor, G. L., "Numerical Solution of Two-Dimensional Turbulent Separated Flows Using a Reynolds Stress Closure Model," *Journal of Fluids Engineering*, Vol. 107, 1985, pp. 467–476.

[6]Arnal, M., and Friedrich, R., "The Instantaneous Structure of a Turbulent Flow over a Backward Facing Step," *Separated Flows and Jets, IUTAM Symposium*, Springer-Verlag, Berlin, 1991, pp. 709–717.

[7]Neto, S., Grand, D., and Lesieur, M., "Simulation numérique bidimensionnelle d'un écoulement turbulent stratifié derrière une marche," *International Journal of Heat and Mass Transfer*, Vol. 34, No. 8, 1991, pp. 1999–2011.

[8]Ffowcs Williams, J. E., and Hall, L. H., "Aerodynamic Sound Generation by Turbulent Flow in the Vicinity of a Scattering Half Plane," *Journal of Fluid Mechanics*, Vol. 40, No. 4, 1970, pp. 657–670.

[9]Howe, M. S., "Contributions to the Theory of Aerodynamic Sound, with Application to Excess Jet Noise and the Theory of the Flute," *Journal of Fluid Mechanics*, Vol. 71, No. 4, 1975, pp. 625–673.

[10]Howe, M. S., "A Review of the Theory of Trailing Edge Noise," *Journal of Sound and Vibration*, Vol. 61, No. 4, 1978, pp. 437–465.

[11]Crighton, D. G., and Leppington, F. G., "On the Scattering of Aerodynamic Noise," *Journal of Fluid Mechanics*, Vol. 46, No. 3, 1971, pp. 577–597.

[12]Meecham, W. C., "Aerosound from Corner Flow and Flap Flow," *AIAA Journal*, Vol. 21, No. 2, 1983, pp. 228–234.

[13]Gradoz, V., Guerder, J. Y., and Jacob, M. C., "Sound Radiated by Plane Wall Jets," *Acustica*, Vol. 82, Suppl. 1, 1996, p. 170.

[14]Schneider, and Goldstein, R. J., "Laser Doppler Measurement of Turbulence Parameters in a Two-Dimensional Plane Wall Jet," *Physics of Fluids*, Vol. 6, No. 9, 1994, pp. 3116–3129.

[15]Jacob, M. C., Gradoz, V., Louisot, A., Juve, D., and Guerrand, S., "Comparison of Sound Radiated by Shallow Cavities and Backward Facing Steps," AIAA Paper 99-1892, May 1999.

[16]Zoppellari E., "Sound Source Localization in Supersonic Jets," *Acustica*, Vol. 82, Suppl. 1, 1996, p. 172.

[17]Tailland, A., and Mathieu, J., "Jet Pariétal," *Journal de Mécanique*, Vol. 6, No. 1, 1967, pp. 103–131.

[18]Kuehn, D. M., "Effects of Adverse Pressure Gradient on the Incompressible Reattaching Flow over a Rearward-Facing Step," *AIAA Journal*, Vol. 38, No. 3, 1980, pp. 41–51.

M. Samimy
Associate Editor